Available online at www.sciencedirect.com
SCIENCE DIRECT
International Journal of Heat and Mass Transfer 49 (2006) 4033–4042
International Journal of HEAT and MASS TRANSFER
www.elsevier.com/locate/ijhmt

Mechanistic study for the interfacial area transport phenomena in an air/water flow condition by using fine-size bubble group model

B.G. Huh [a,*], D.J. Euh [b], H.Y. Yoon [b], B.J. Yun [b], C.-H. Song [b], C.H. Chung [a]

[a] Department of Nuclear Engineering, Seoul National University, Shinlim-Dong, Gwanak-Gu, Seoul 157-742, Republic of Korea
[b] Korea Atomic Energy Research Institute, P.O. Box 105, Yuseong, Daejeon 305-600, Republic of Korea

Received 14 September 2005
Available online 9 June 2006

Abstract

A set of number density transport equations based on the bubble size are used to predict the void fraction and the interfacial area concentration in an air/water flow conditions. As the closure relations for the number density transport equations, a coalescence due to random collisions and a breakup due to an impact of the turbulent eddies are modified based on previous studies. The bubble expansion term due to a pressure reduction and a coalescence due to a wake entrainment are modeled for the number density transport equation. In order to predict the local experimental data, a computational fluid dynamic (CFD) code coupling the two-fluid model and number density transport equations are developed in this study. As for the results of the numerical analysis, the developed model predicts well the void fraction and interfacial area concentration although some deviations between the prediction and the experiment are shown for the high void fraction conditions.

Keywords: Number density; Interfacial area; Void fraction; Two-fluid model; Coalescence; Breakup

1. Introduction

In the state of the art models, the two-fluid model is considered as the most detailed and accurate macroscopic formulation of the thermo-fluid dynamics of the two-phase systems. In the formulation of a two-fluid model, appropriate constitutive relations for the interfacial transfer terms are required to close the phasic balance equations [1]. In general, the interfacial transfer terms are proportional to the interfacial area concentration (IAC), which is defined as the interface area per unit fluid volume. Therefore, the interfacial area concentration is one of the most important parameters in a two-fluid model.

The empirical correlations for the interfacial area concentration are being used in the current system codes such as RELAP5, TRAC, CATHARE and MARS. Since the empirical correlations strongly depend on the flow regimes map, they have the feature of a discontinuity at the flow regime transition and can cause a bifurcation problem in the two-phase models. Furthermore, because most of the empirical correlations assume the steady state and fully developed flow conditions, they are hard to be applied for developing conditions including the entrance effect or transient systems [2]. In order to overcome the weakness of the empirical correlation methods, mechanistic approaches by using transport equations for the interfacial area concentration or particle number density have been proposed [2–9]. Most of the mechanistic studies are mainly classified into one-group and two-group methods. Since a one-group method assumes a uniform size of the particles, it can effectively predict the interfacial area concentration in a dispersed flow regime where the particle size is small and shapes are identical. For the cap or slug flow conditions, a two-group model has been developed by separating the particle size and hydraulics for each bubble group [2,9–11]. Although the two-group method can be applied to various flow regimes including flow regime transitions, it requires

* Corresponding author. Tel.: +82 2 875 8868; fax: +82 2 889 2688.
E-mail address: huha@snu.ac.kr (B.G. Huh).

0017-9310/$ - see front matter © 2006 Elsevier Ltd. All rights reserved.
doi:10.1016/j.ijheatmasstransfer.2005.11.037

Nomenclature

a_i	local interfacial concentration
A_i	surface area of the bubble in a bubble group i
C_{RC}, C_{WE}, C_{BR}	adjustable parameters in the bubble interaction models
D_T	pipe diameter
D	bubble diameter
D_c, D_s	boundary size of the cap and slug bubbles
$d_{daughter,max}$	diameter of the maximum daughter bubble
d_L	diameter of the leading bubble
E_{eddy}	eddy energy
E_S	surface tension energy
f_i	probability density of a bubble group i
L_W	wake length
n_e	number density of the eddy
n_i	number density of a bubble group i
r_{ij}	equivalent radius
S_{ie}	collision cross-sectional area
t	time
t_{ij}	time required for a coalescence of the bubbles
$\bar{u}$	mean bubble velocity
V_a	volume available for a collision
V_i	bubble volume of a bubble group i
V_{max}	maximum bubble volume
V_{min}	minimum bubble volume
z	characteristic distance ($= y/L_W$)

Greek symbols

ε	energy dissipation
Γ_{ij}, Γ_{ie}	coalescence and breakup rate
λ_{ij}, λ_{ie}	collision efficiency in the coalescence and breakup efficiency in the breakup
λ_{min}, λ_{max}	minimum and maximum eddy size
ρ	density
σ	surface tension
τ_{ij}	contact time for the bubbles

Subscripts

f	liquid phase
g	gas phase
i, j, k	bubble size group
l	leading bubble
ncap	minimum cap bubble size group
t	trailing bubble

more constitutive relations for the particle interactions than the one-group method.

In the mechanistic modeling of the interfacial area concentration, the particle size is predicted by modeling the bubble interactions such as the breakup and coalescence process of the particles [12]. Also, a particle expansion/contraction due to a pressure variation influences on the variation of the particle size. This leads to the so-called population balance equation. The number density transport equation is obtained by integrating the population balance equation over the volume of all the sizes of the particles. In most studies which are described above, the detailed particle volume dependent number density equation is considered as being too complicated for use in the field equations. But, a more detailed particle size effect should be considered because the particle size influences the inter-phase heat and mass transfer through the IAC and the momentum drag terms.

In this study, in order to consider the effect of the particle size in more detail, the number density transport equations for a number of particle size groups (11–16 size groups) are used in an analysis of the air/water flow system. In order to constitute the number density transport equation, the bubble expansion/contraction term and a coalescence due to a wake entrainment are developed and the coalescence due to a random collision and the breakup due to an impact of the turbulent eddies are modified based on previous studies. The multi-dimensional computational fluid dynamics (CFD) code is developed by coupling systematically the two-fluid model with the number density transport equation of each size group. To validate the developed code and the number density transport equation, comparisons of the void fraction and IAC for various flow conditions are performed against local experimental data in an air/water loop [13]. The contribution of the bubble interaction terms for the interfacial area concentration is also analyzed.

2. Experimental facilities

In order to obtain the two-phase parameters such as the void fraction, interfacial area concentration and Sauter mean diameter etc., the experiments are performed in an air/water test loop which is installed at the Korea Atomic Energy Research Institute (KAERI) as shown in Fig. 1.

The test loop consists of a test section, bubble generator, water supply system, air supply system and a data acquisition system. The test section is made of transparent acryl pipe where the diameter is 0.08 m and the height is about 10 m. The test section is composed of the conductivity probe spoolpieces for measuring the local gas velocity, void fraction and interfacial area concentration, and the impedance void meter spoolpieces for measuring the channel averaged void fraction. A five-sensor conductivity probe is applied to measure the local flow parameters [14,15]. In this experiment, the superficial liquid velocity is varied from 0.5 m/s to 2.0 m/s and the superficial gas velocity is changed from 0.100 m/s to 0.698 m/s at the first measuring position of the test section as shown in Fig. 2. The experimental data for the conductivity probe is obtained locally

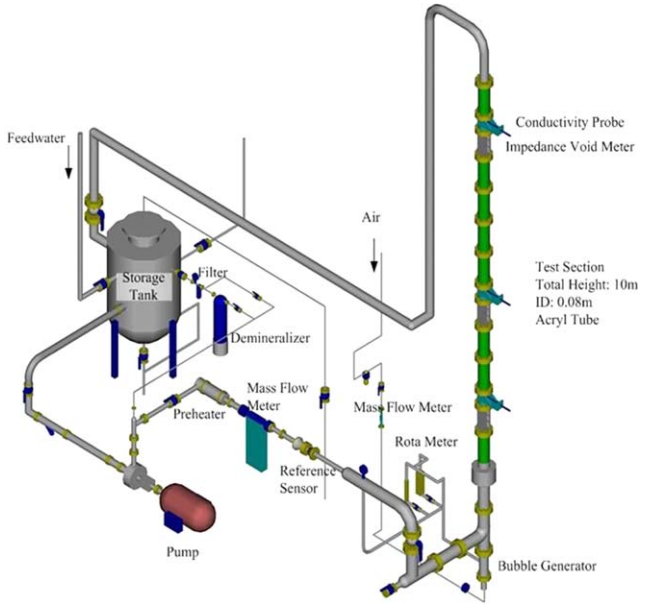

Fig. 1. The air/water test loop.

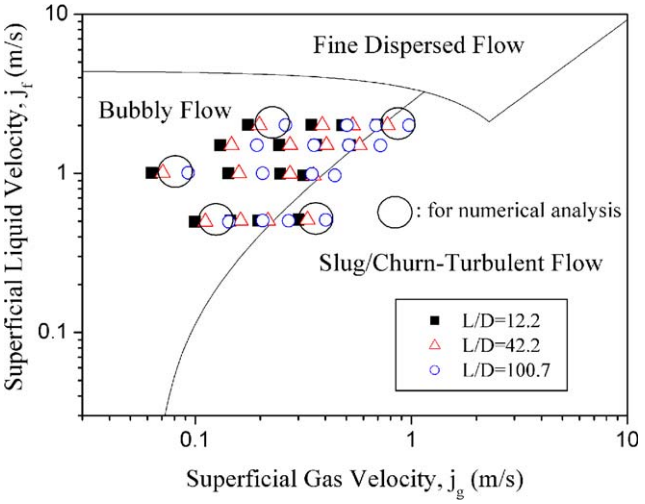

Fig. 2. The experimental flow conditions.

at 16 measuring points along the radial direction. Sixteen measuring points are equally spaced from the centerline of the test section. The experimental data, which includes from the bubbly flow regime to the churn turbulent/slug flow regime, is produced at three axial positions $L/D =$ 12.2, 42.2 and 100.7 and the investigation for the transport phenomena of the flow parameters is performed at three axial positions. The experimental temperature is about 30 °C. The pressure is about 2 bar at the inlet of the test section.

3. Number density transport equation

In this study, the number density transport equations for each bubble group are applied to predict the two-phase flow parameters such as the interfacial area concentration and the void faction. Based on the study of Prince et al. [16], the coalescence and breakup models are modified by considering a proper physical approach. A wake entrainment model is developed to apply it to the number density transport equation.

The number density transport equation is obtained by integrating the transport equation of the number probability density function over the volume of all the particle sizes:

$$\frac{\partial n_i}{\partial t} + \nabla \cdot (\vec{u}_g n_i) = \frac{\vec{u}_g}{\rho_g} \cdot \nabla \rho_g \cdot \int \left(V \frac{\partial f}{\partial V} + f \right) dV + S_{i,C} + S_{i,B} + S_{i,W} \quad (1)$$

where f, n_i, $\vec{u}_g$ and ρ_g are the probability density of bubbles, number density, gas velocity and gas density. $S_{i,C}$, $S_{i,B}$ and $S_{i,W}$ are the source and sink terms of the bubble coalescence, breakup and wake entrainment respectively. The first term of the right-hand side of Eq. (1) considers a gas expansion due to changes in the gas density along the bubble path. The expansion term of the gas phase has to be included when the gas density changes considerably such as this study and is expressed as follows:

$$\frac{\vec{u}_g}{\rho_g} \cdot \nabla \rho_g \cdot \int \left(V \frac{\partial f}{\partial V} + f \right) dV = \frac{\vec{u}_g}{\rho_g} \cdot \nabla \rho_g \cdot (Vf)_{V_{i-1/2}}^{V_{i+1/2}} = \frac{\vec{u}_g}{\rho_g} \cdot \nabla \rho_g \cdot (f_{i+1/2} V_{i+1/2} - f_{i-1/2} V_{i-1/2}) \quad (2)$$

where $f_{i+1/2} \cong \frac{f_i + f_{i+1}}{2}$, $f_{i-1/2} \cong \frac{f_{i-1} + f_i}{2}$ and $f_i \cong \frac{n_i}{\Delta V_i} = \frac{n_i}{V_{i+1/2} - V_{i-1/2}}$.

3.1. Bubble coalescence due to random collisions

A bubble coalescence is considered to occur due to a random collision driven by the turbulence of a liquid phase. A coalescence of two bubbles is induced in the following processes: (1) bubbles collide, (2) a small amount of the liquid between the bubbles is trapped and drains gradually, (3) the liquid film between the bubbles reaches a critical thickness and a film rupture occurs resulting in a coalescence. Based on the study of Prince et al. [16], the source and sink terms of the number density which is induced by a bubble coalescence due to a random collision can be expressed by the following equations respectively:

$$S_{i,C}^{source} = \frac{1}{2} \sum_{k=1}^{N} \sum_{l=1}^{N} \Gamma_{i,kl} \begin{cases} \Gamma_{i,kl} = \Gamma_{kl} & V_{i,\min} \leqslant V_k + V_l \leqslant V_{i,\max} \\ \Gamma_{i,kl} = 0 & V_k + V_l > V_{i,\max} \\ & \text{or } V_k + V_l < V_{i,\min} \end{cases} \quad (3)$$

$$S_{i,C}^{sink} = \sum_{j=1}^{N} \Gamma_{ij}$$

where Γ_{ij}, N, V_{min}, V_{max} and V are the coalescence rates of the bubbles of group i and group j, total bubble group, minimum bubble volume, maximum bubble volume and mean bubble volume for each group respectively. The subscripts indicate the bubble group. In the production term, since the factor 1/2 is considered to avoid a counting of

the coalescence events twice, the factor should be neglected in the case of a collision between bubbles in the same group ($k = l$).

The bubble coalescence rate Γ_{ij} can be expressed in terms of the collision rate θ_{ij} and the collision efficiency λ_{ij}. The collision rate can be given as a function of the number density, collision area and the bubble relative velocity [16]. In this study, the relative velocity is considered as the difference of the velocity for the approaching two bubbles with an opposite direction. The coalescence efficiency is expressed as a function of the time required for a coalescence of the bubbles t_{ij} and the contact time for the two bubbles τ_{ij} [17]. The coalescence time and the contact time that were derived respectively by Kirkpatrick and Lockett [18] and Levich [19] are used. From the above descriptions, the coalescence rates of the bubble i and the bubble j are obtained as follows:

$$\Gamma_{ij} = C_{\mathrm{RC}} \cdot n_i n_j \cdot (d_i + d_j)^2 \cdot \varepsilon^{1/3} \cdot \left| d_i^{1/3} + d_j^{1/3} \right| \cdot \exp\left(-\frac{\rho_{\mathrm{f}}^{1/2} r_{ij}^{5/6} \varepsilon^{1/3}}{\sigma^{1/2}} \right) \tag{4}$$

where d, $r_{ij}^{-1} = 0.5(r_i^{-1} + r_j^{-1})$, ε, ρ_{f} and σ are the bubble diameter, equivalent radius, energy dissipation, liquid density and the surface tension, respectively.

3.2. Bubble breakup due to the impact of turbulent eddies

A bubble breakup is induced by a collision with a turbulent eddy of a similar size to the bubble. From previous studies [9,16], the main parameter inducing a bubble breakup can be considered as the energy and size of the eddy. When the Reynolds number is large enough, a large eddy usually transports the bubble. For this reason, daughter bubbles formed from a breakup have a smaller size than the length scale of the eddy. On the contrary, a very small eddy does not have enough energy to break a bubble. Therefore, the eddy size for a breakup can be determined as slightly smaller than or equal to the bubble. Based on the study of Prince et al. [16], the source and sink terms of the number density which is induced by a bubble breakup due to an impact of turbulent eddies can be expressed by the following equations respectively:

$$\begin{aligned} S_{i,\mathrm{B}}^{\mathrm{source}} &= \sum_{j=i+1}^{N} \Gamma_{j,i\mathrm{e}} \begin{cases} \Gamma_{j,i\mathrm{e}} = \Gamma_{i\mathrm{e}} & V_j + V_0 = V_i \\ \Gamma_{j,i\mathrm{e}} = 0 & V_j + V_0 \neq V_i \end{cases} \\ S_{i,\mathrm{B}}^{\mathrm{sink}} &= \sum_{j=1}^{i-1} \Gamma_{j,i\mathrm{e}} \end{aligned} \tag{5}$$

where V_i and V_0 are the volume of the two daughter bubbles, respectively. V_j denotes the mother bubble and the subscript indicates the bubble group.

The bubble breakup rate $\Gamma_{j,i\mathrm{e}}$, which is analogous to the coalescence rate, is given as a function of the collision rate and the breakup efficiency. The breakup efficiency is expressed by the function of the surface energy and the eddy energy and it indicates the fraction of the turbulent eddies colliding with the bubble that a turbulent kinetic energy greater than the surface tension energy of the bubble. From the previous studies [16,17], the breakup rate of the group i bubble into the group j bubble after colliding with the eddy:

$$\Gamma_{j,i\mathrm{e}} = C_{\mathrm{BR}} \cdot n_i n_{\mathrm{e}} \varepsilon^{1/3} \left(d_i^{1/3} + \frac{d_i^{4/3} - \lambda_{\min}^{4/3}}{d_i - \lambda_{\min}} \right) S_{i\mathrm{e}} \cdot \exp\left(-\frac{E_{\mathrm{S}}}{E_{\mathrm{eddy}}} \right) \tag{6}$$

where n_{e}, $E_{\mathrm{eddy}} \approx \int_{\lambda_{\min}}^{d_i} \rho_{\mathrm{f}} \lambda^{11/3} \varepsilon^{2/3} \, \mathrm{d}\lambda / \int_{\lambda_{\min}}^{d_i} \mathrm{d}\lambda$, $E_{\mathrm{S}} \approx \sigma(d_j^2 + d_0^2 - d_i^2)$, $S_{i\mathrm{e}} \approx \int_{\lambda_{\min}}^{d_i} (d_i + \lambda)^2 \, \mathrm{d}\lambda / \int_{\lambda_{\min}}^{d_i} \mathrm{d}\lambda$ and $\lambda_{\min}$ are the eddy number density, the eddy energy, the surface tension energy, the area of breakup and the minimum eddy diameter for a breakup, respectively.

In this study, since it is assumed that only an eddy with a length smaller than or equal to the breaking bubble [20], the maximum eddy size is chosen as follows:

$$\lambda_{\max} = d_i \tag{7}$$

The minimum eddy size is chosen as the following equation by considering an assumption that only daughter bubbles with a diameter smaller than the length scale of the eddy can be formed [21]:

$$\lambda_{\min} = d_{\mathrm{daughter,max}} = \max(d_j, d_0) \tag{8}$$

where d_i, d_0 and d_j are the diameter of the mother bubble and the diameters of the two daughter bubbles, respectively. The relation of these diameters is denoted as follows: $d_0 = (d_i^3 - d_j^3)^{1/3}$.

3.3. Bubble coalescence due to a wake entrainment

The wake entrainment is a phenomena where the trailing bubble accelerates and coalescences with the leading one when the bubble enters the wake region of a leading large bubble as shown in Fig. 3. When the leading bubble is large, a circular wake is formed behind the large leading bubble. This wake is considered as a mixing region with a high level of turbulence. The liquid velocity fluctuation behind the leading bubble influences the shape and behavior of the trailing bubble. Therefore, the wake length and the velocity profile in the wake are important for describing the nature of this mechanism. In this study, the coalescence terms due to a wake entrainment are developed to apply them to the number density transport equation. The source and sink terms of the number density which are induced by a bubble coalescence due to a wake entrainment can be expressed by the following equations, respectively:

$$\begin{aligned} S_{i,\mathrm{W}}^{\mathrm{source}} &= \sum_{k=\mathrm{ncap}}^{N} \sum_{l=1}^{k-1} \Gamma_{i,kl} \begin{cases} \Gamma_{i,kl} = \Gamma_{kl} & V_{i,\min} \leqslant V_k + V_l \leqslant V_{i,\max} \\ \Gamma_{i,kl} = 0 & V_k + V_l > V_{i,\max} \\ & \text{or } V_k + V_l < V_{i,\min} \end{cases} \\ S_{i,\mathrm{W}}^{\mathrm{sink}} &= \begin{cases} \sum_{j=\mathrm{ncap}}^{N} \Gamma_{ji} & i < \mathrm{ncap} \\ \sum_{j=1}^{i-1} \Gamma_{ij} + \sum_{j=i+1}^{N} \Gamma_{ji} & i > \mathrm{ncap} \end{cases} \end{aligned} \tag{9}$$

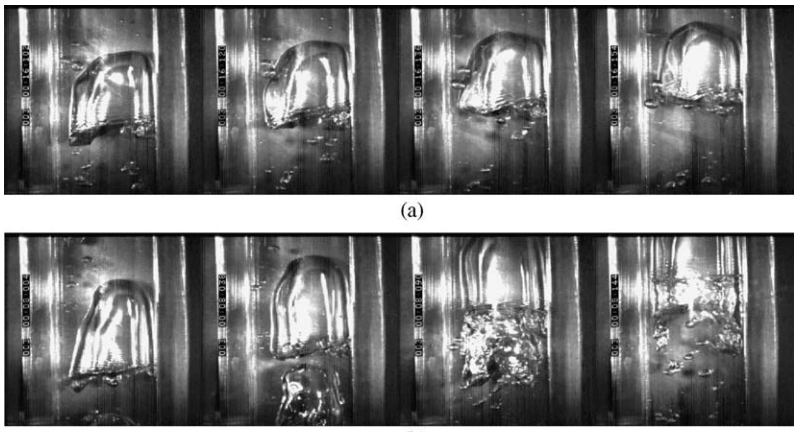

Fig. 3. The wake entrainment. (a) An interaction with small trailing bubble and (b) an interaction with large trailing bubble.

where ncap is the minimum cap bubble size group. The subscripts indicate the bubble group.

In this study, the wake entrainment is considered when the leading bubble is only a cap or slug bubble and the boundary of the cap and the slug bubble can be determined respectively by [4,21]:

$$D_c = 4\sqrt{\frac{\sigma}{g\,\Delta\rho}} \sim 1\ \text{cm}, \quad D_s = 40\sqrt{\frac{\sigma}{g\,\Delta\rho}} \sim 10\ \text{cm} \tag{10}$$

where g, $\Delta\rho$ and σ are the acceleration due to gravity, a difference in the density between the phases and the surface tension, respectively. Therefore, when the mean diameter of any group is larger than 1 cm, the bubble of that group can be considered as the leading bubble.

The coalescence rate Γ_{ij} due to a wake entrainment can be expressed in terms of the collision rate θ_{ij} and the collision efficiency λ_{ij}. The collision rate can be given as a function of the relative velocity and the number density of each group as below:

$$\theta_{ij} = n_i n_j V_a \frac{|\bar{u}_t - \bar{u}_l|}{d_{m,path}} \tag{11}$$

where V_a, $\bar{u}_t$, $\bar{u}_l$ and $d_{m,path}$ are the volume available for a collision, velocity of the trailing and leading bubble and the mean free path of the trailing bubble, respectively.

The volume available for a collision between the leading bubble and the trailing one is expressed as the projected bubble area multiplied by the wake:

$$V_a = \frac{\pi}{4} d_L^2 \cdot L_W \tag{12}$$

where d_L and L_W are the diameter of the leading bubble and the wake length, respectively. For the cap bubbles, Miyahara et al. [22] proposed experimentally that the wake length was $5d_L \sim 8d_L$ when the bubble diameter is smaller than the pipe size. In this study, the wake length of the cap bubble is chosen as $6.5d_L$. For the slug bubbles, Pinto et al. [23] found experimentally that the wake length was about five times as large as the flow channel diameter ($\sim 5D_T$) when the liquid flow regime was either laminar or turbulent.

The collision rate is proportional to the relative velocity between the leading bubble and the trailing one. The velocity relation of the two bubbles can be obtained irrespective of the liquid flow pattern behind a slug [24]:

$$\frac{\bar{u}_t}{\bar{u}_l} = -11.4\frac{y}{L_W} + 4.24 \quad \text{for } \frac{y}{L_W} < 0.24 \tag{13}$$

$$\frac{\bar{u}_t}{\bar{u}_l} = 2.01 - 1.96\frac{y}{L_W} + 0.96\left(\frac{y}{L_W}\right)^2 \quad \text{for } 0.24 < \frac{y}{L_W} < 1 \tag{14}$$

where y is a distance between the leading and trailing bubble. Eqs. (13) and (14) are applied to both the cap and slug leading bubbles in this study.

Therefore, the relative velocity between the leading and trailing bubble can be obtained by using Eqs. (11), (13) and (14):

$$\begin{aligned} |\bar{u}_t - \bar{u}_l| &= \bar{u}_l\left|\frac{\bar{u}_t}{\bar{u}_l} - 1\right| = \bar{u}_l \int_0^1 \left|\frac{\bar{u}_t}{\bar{u}_l} - 1\right| dz \\ &= \bar{u}_l \int_0^{0.24} |-11.4z + 3.24|\, dz + \bar{u}_l \\ &\quad \times \int_{0.24}^1 |0.96z^2 - 1.96z + 1.01|\, dz \\ &= 0.608 \cdot \bar{u}_l \end{aligned} \tag{15}$$

where z is the characteristic distance which is expressed by y/L_W.

The velocity of the leading bubble $\bar{u}_l$ can be considered as the individual cap or slug bubble velocity in a column. For the cap bubbles, Krishna et al. [25] proposed the velocity of a cap bubble in the size range $D = 3$–80 mm from the results of an extensive experimental investigation:

$$\begin{aligned} &\bar{u}_l = \sqrt{g d_L/2} \cdot SF \quad \text{for } d_L > 0.017 \\ &SF = 1 \quad \text{for } \frac{d_L}{D_T} < 0.125 \\ &SF = 1.13\exp\left(-\frac{d_L}{D_T}\right) \quad \text{for } 0.125 < \frac{d_L}{D_T} < 0.6 \\ &SF = 0.496\sqrt{D_T/d_L} \quad \text{for } \frac{d_L}{D_T} > 0.6 \end{aligned} \tag{16}$$

For the slug bubbles, the velocity of the slug bubble through a stagnant liquid can be given as a function of the acceleration due to gravity, g and the internal diameter of the tube, D_T as follows:

$$\bar{u}_l = 0.35(gD_T)^{1/2} \tag{17}$$

If the probability of a trailing bubble existing along the wake length has the same value, the mean free path of the trailing bubble can be obtained as a simple equation:

$$d_{m,path} = \frac{\int_0^{L_W} y\,dy}{\int_0^{L_W} dy} = \frac{L_W}{2} \tag{18}$$

where L_W and y are the wake length and the distance from the base of the leading bubble, respectively. The collision rate becomes larger as the mean free path of the trailing bubble decreases.

The coalescence efficiency for a wake entrainment which is analogous to a bubble coalescence due to random collisions, can be expressed as a function of the time required for a coalescence of the bubbles t_{ij} and the contact time for two bubbles τ_{ij}. However, in the coalescence time, the interaction for the bubbles with a similar size is considered as a main contribution in the coalescence due to a random collision. On the contrary, in the wake entrainment, the interaction between small bubbles and large bubbles is considered as more important. The small bubble collides with the base of the large bubble and two bubbles coalescence after fully draining the liquid film. Therefore, this phenomenon can be considered as not the interaction of the bubbles with a similar size but the interaction of a bubble and an interface when the base of the large bubble is assumed as a flat interface without an oscillation. In order to obtain the coalescence time for a wake entrainment, the film drainage equation for the bubble-interface interaction which was derived by Kirkpatrick and Lockett [18] is used in this study. From the above descriptions, the coalescence rates due to a wake entrainment of bubble group i and bubble group j can be obtained by the following equation:

$$\Gamma_{ij} = C_{WE} \cdot n_i n_j d_i^2 \bar{u}_i \cdot \exp\left(-\frac{\rho_f^{1/2} r_{ij}^{5/6} \varepsilon^{1/3}}{\sigma^{1/2}}\right) \tag{19}$$

where C_{WE} is an adjustable parameter that can be evaluated with experimental data.

4. Numerical analysis

In this study, a multi-dimensional code is set up by using the two-fluid model and the number density transport equation for each bubble group. The flow fields of the fluid are calculated using the two-fluid model and the local parameters such as the void fraction and IAC are computed by the number density transport equation. The two-fluid model and the number density transport equation are coupled systematically with each other. Two sets of the conservation equations of the mass and momentum are applied to liquid and gas phases, respectively. The constitutive relations such as the drag force, virtual mass force and lift force are included for the calculation of interface momentum transfer. The governing equations are discretized using the finite volume method (FVM), where the equations are integrated for structured or unstructured grids. An incompressible fluid is assumed and the discretized equations are solved using the simplified marker and cell (SMAC) algorithm [26]. All the variables such as the pressure and velocity are defined at the cell center. The linear sets of the equations obtained from the pressure calculation are computed by a conjugate gradient solver.

The flow field of gas phase calculated from the momentum equation is applied to the number density transport equations. Currently, since the bubble velocity is simplified from an assumption that all bubbles are moving at the same velocity, the same velocity profile for bubble is used for each bubble group. The void fraction and interfacial area concentration obtained from the number density transport equations are used for the flow field calculation. The calculation is carried out for 11–16 bubble size groups in the conditions as shown in Table 1.

Table 1
The experimental flow conditions for the numerical analysis

	Superficial liquid velocity (m/s)	Void fraction	Remarks	Number of bubble groups for the calculation
Case01	Low (0.5)	Low (10%)	Core peaking, bubbly flow	14
Case02	Low (0.5)	High (24%)	Core peaking, **slug flow**	16
Case03	Intermediate (1.0)	Low (5%)	**Wall peaking**, bubbly flow	11
Case04	High (2.0)	Low (6%)	Core peaking, bubbly flow	14
Case05	High (2.0)	High (20%)	Core peaking, **slug flow**	15

5. Results and discussion

In order to evaluate the number density transport equations and the developed code, a comparison of the prediction with the experimental data generated in the air/water loop is performed. For an assessment of the void fraction and the interfacial area concentration at the local points, five flow conditions are chosen by considering the liquid velocity, void fraction and flow pattern as shown in Table 1 and Fig. 2. In this study, most experiments show the core peaking for a void fraction. Since only two cases, which are Case03 and Case04, show the wall peaking for a void fraction, these are chosen for the numerical analysis. The experimental data at the two upper axial positions $L/D =$ 42.2 and 100.7 is used because an entrance effect of bubble generator is small if possible. The axial distance between the two positions is 4.68 m. The experimental data at $L/D = 42.2$ is used as input and the prediction results

which are obtained at $L/D = 100.7$ are compared with the experimental data.

Figs. 4–7 show the comparative results of the void fraction and the interfacial area concentration for the five cases. In order to evaluate the capability of the developed code and model in analyzing a general two-phase flow, the adjustable parameter of each bubble interaction model is used with the same value for the five cases irrespective of its flow regime or characteristic of the radial bubble distribution. The adjustable parameter of each bubble interaction model is given as follows:

$$C_{RC} = 0.005, \quad C_{WE} = 0.005 \quad \text{and} \quad C_{BR} = 0.005 \qquad (20)$$

Figs. 4 and 5 show the results of the void fraction and interfacial area concentration, respectively, for Case01, Case02 and Case03. In Case01 where the liquid velocity and void fraction are low, the core peaking is predicted well and the void fraction and the interfacial area concentration are also predicted well and the relative errors are 18.1% and 8.8%, respectively. On the contrary, in Case02 where the liquid velocity is low and the void fraction is high, the core peaking is clearly shown but the void fraction and the interfacial area concentration predicted by the developed code and model have large relative deviations. Since the void fraction is proportional to the interfacial area concentration, the error trend of the void fraction is similar to that of the interfacial area concentration. In this condition which is included in a slug flow regime, since the interval of the mean bubble diameter between the bubble groups is large due to the large bubbles, large errors can occur in evaluating the bubble interactions between the bubble groups. Therefore, if the number of the bubble groups is larger than that in this calculation, the relative error can be further reduced. However, since large bubble groups increase the calculation time, the number of the bubble groups should be selected carefully by considering both effects. In general, the measuring error is large near to

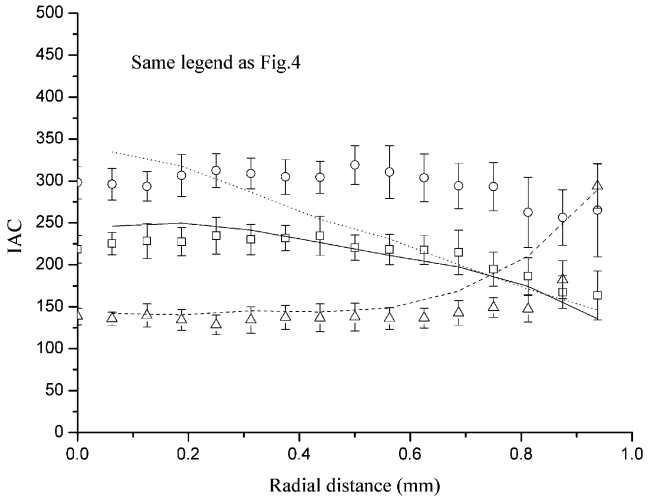

Fig. 5. Comparison of the predicted and measured IAC (Case01, Case02 and Case03).

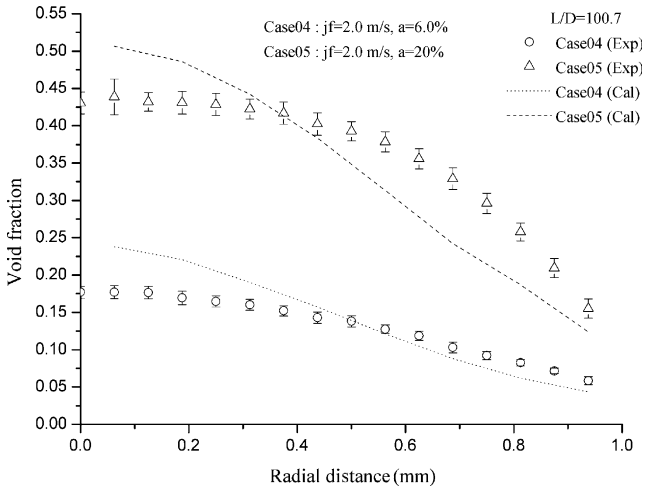

Fig. 6. Comparison of the predicted and measured void fraction (Case04 and Case05).

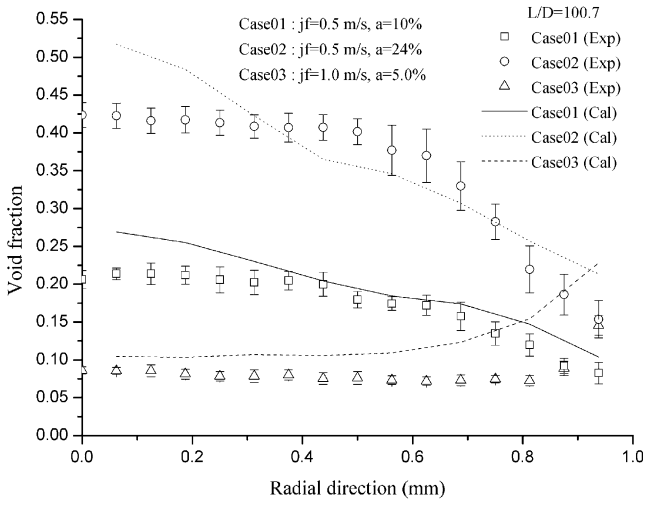

Fig. 4. Comparison of the predicted and measured void fraction (Case01, Case02 and Case03).

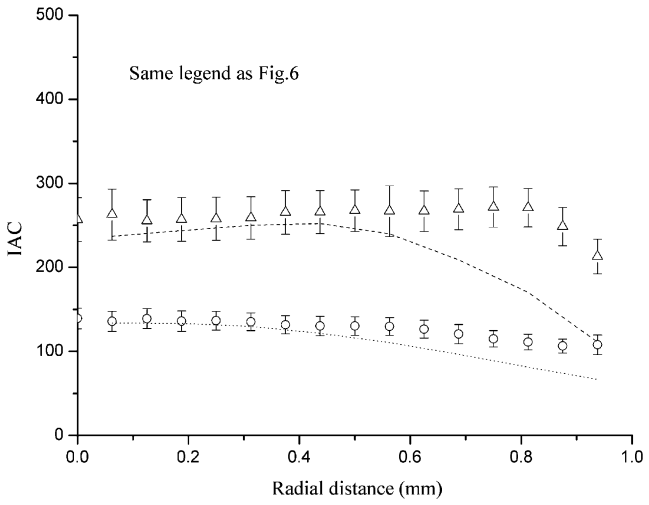

Fig. 7. Comparison of the predicted and measured IAC (Case04 and Case05).

the wall because the undesirable phenomena can occur from the disturbed flow and the interfacial area concentration can be overestimated by the steep interfaces in the condition where a large slug occupies the entire flow channel diameter. Therefore, the possibility of a large experimental error can be considered as an explanation for the disagreement of the interfacial area concentration in a region which is close to the wall. Also, since the interfacial forces that are used in the two-fluid model were developed by considering the one-dimensional concept and the drag coefficient of a slug flow regime is a function of only the void fraction regardless of the bubble diameter, the predictive error may be large in this condition which is a slug flow regime. The relative errors of the void fraction and the interfacial area concentration are 18.6% and 26.0%, respectively. In Case03, the wall peaking is predicted well. The local prediction results for the void fraction and the interfacial area concentration predict well the trends of the experimental data but the relative deviation for the void fraction is somewhat large in the region that is near to the wall. In general, the lift, wall-lubrication and turbulent dispersion forces affect the radial distribution of the void fraction. In this study, since the lift force is only considered, the relative deviation for the void fraction can be large in a region which is close to the wall. If the wall-lubrication and turbulent dispersion forces were to be included in the developed code, the predictive capability for the void fraction may be advanced. The relative errors of the void fraction and the interfacial area concentration are 58.2% and 17.2%, respectively.

Figs. 6 and 7 show the prediction results of the void fraction and the interfacial area concentration, respectively for Case04 and Case05. In Case04 where the liquid velocity is high and the void fraction is low, the core peaking is illustrated well as shown in Fig. 6 and the void fraction and interfacial area concentration are predicted well by the developed code. The relative errors for the void fraction and interfacial area concentration are 22.5% and 18.9%, respectively. In Case05 where the void fraction is high and the liquid velocity is high, the flow condition is located in the slug flow regime. The core peaking is shown well but the void fraction does not predict well the local experimental data. The interfacial area concentration follows the trend of the experimental data at the central region but a large deviation is shown in the region which is close to the wall. The causes of a difference between the predictive and experimental results can be proposed as those described for Case02. The relative errors for the void fraction and the interfacial area concentration are 18.0% and 23.5%, respectively.

As shown in Figs. 4–7, although the relative deviations are large in the flow conditions which are included in the slug flow regime, the predictive capability of the developed model and code for the void fraction and interfacial area concentration is acceptable in most flow conditions. In flow conditions (Case01 and 04) where the void fraction is low and they are included in the bubbly flow regime, the agreement between the model prediction and the experimental data is remarkable. Also, in flow condition (Case03) where there is a wall peaking, the predictive results show well the trends of the experimental data.

In order to investigate the contribution for the interfacial area concentration from each bubble interaction term and its sensitivity to the flow conditions, the estimation for each bubble interaction term is shown in Figs. 8 and 9. Since the number density for each bubble group is related to that of the entire neighboring cells in the multi-dimensional condition and it is varied due to the convection for the axial and radial directions and the bubble interaction terms, it is difficult to accurately understand the variation of the number density due to each bubble interaction term along the flow path. Therefore, the contribution made by each bubble interaction term is expressed as a ratio for the pressure term, which is shown as the maximum contribution term, by considering a variation of the number density for each bubble interaction term in all the cells. In Fig. 8, the contribution of each bubble interaction term is examined for a condition where the liquid superficial velocity is low.

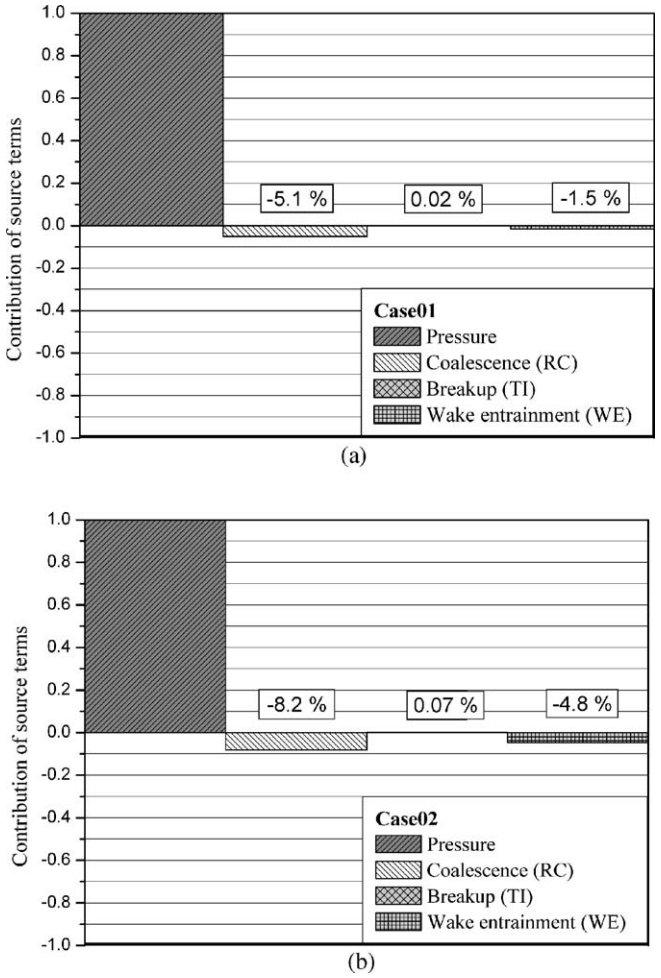

Fig. 8. Contribution of the bubble interaction terms for the IAC variation (Case01 and Case02). (a) Case01 ($j_f = 0.5$ m/s, $\alpha = 10\%$) and (b) Case02 ($j_f = 0.5$ m/s, $\alpha = 24\%$).

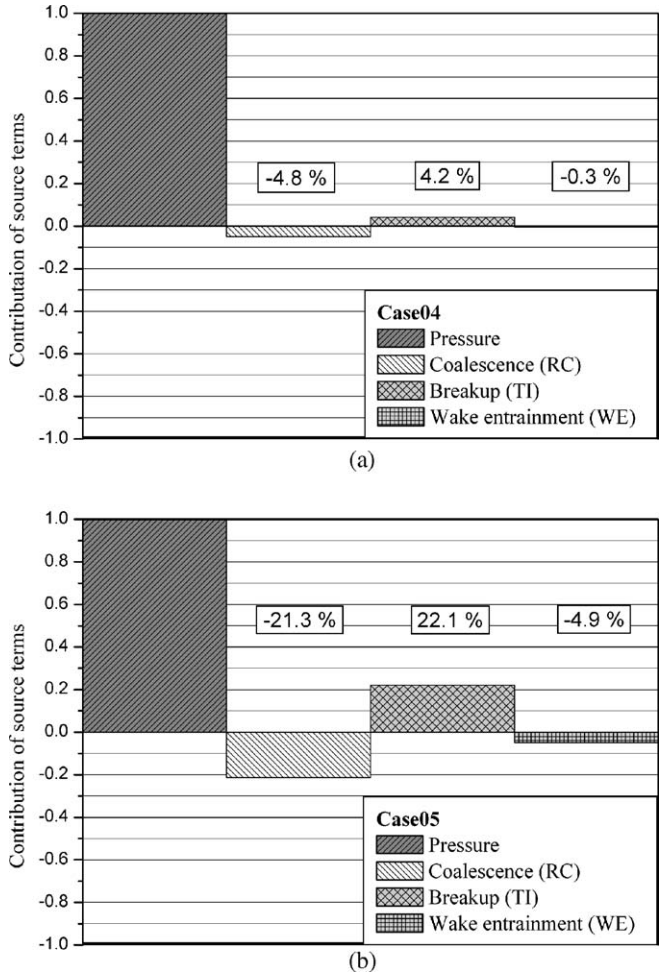

Fig. 9. Contribution of the bubble interaction terms for the IAC variation (Case04 and Case05). (a) Case04 ($j_f = 2.0$ m/s, $\alpha = 6\%$) and (b) Case05 ($j_f = 2.0$ m/s, $\alpha = 20\%$).

In these flow conditions, it can be found that the coalescence due to a random collision (RC) and a wake entrainment (WE) are the dominant mechanisms in the bubble interactions, whereas the breakup due to a turbulent impact (TI) has no role. This is due to the fact that the turbulent energy is not high enough to break the bubbles in these flow conditions. As the void fraction increases, the coalescence due to a random collision (RC) and wake entrainment (WE) become more significant. Therefore, in these flow conditions, a bubble expansion due to a pressure reduction serves as the only source term in a variation of the interfacial area concentration, while a coalescence due to a random collision (RC) and a wake entrainment (WE) serve as sinks.

The contribution from the breakup due to the turbulent impact (TI) becomes evident as the liquid superficial velocity increases. In Fig. 9, the contribution of each bubble interaction term is shown for a condition where the liquid superficial velocity is high. It is clear from the figures that the contribution from the breakup due to the turbulent impact (TI) becomes more significant than that in Fig. 8. As shown in Fig. 9, the coalescence due to a random collision (RC) becomes more important than a wake entrainment (WE). This is due to the increase in the turbulent fluctuations in the flow conditions where the turbulent effect is high. In Case05 where the void fraction is high, all of the bubble interaction terms become more significant and the breakup due to the turbulent impact (TI) and a coalescence due to a random collision (RC) are more dominant terms. Therefore, in these flow conditions, a bubble expansion due to a pressure reduction and the breakup due to a turbulent impact (TI) serve as the source terms in a variation of the interfacial area concentration, while a coalescence due to a random collision (RC) serves as a more dominant sink term when compared to a wake entrainment (WE).

6. Conclusions

A computational fluid dynamics code coupling the two-fluid model and number density transport equations was developed to obtain the flow parameters in a two-phase flow. As the closure relations for the number density transport equations, a coalescence due to random collisions and a breakup due to an impact of the turbulent eddies were modified based on previous studies. The bubble expansion term due to a pressure reduction and a coalescence due to a wake entrainment were also modeled. The coalescence rate due to a wake entrainment was considered when the leading bubble is only cap or slug bubble and the relative velocity between bubbles in a wake was applied using the experimental correlations. The calculation results were compared to that of the experimental study for various conditions. It showed a good agreement between the calculation and the experiment except at the high void fraction conditions. In low void fraction conditions, the calculated results predicted well the trends of the void fraction, interfacial area concentration and the radial bubble distributions. The importance level of the particle interaction mechanisms concerning the flow conditions can be determined by the contribution of the bubble interaction terms. The effect of bubble expansion was shown as the maximum contribution term. In the conditions where the liquid flow is low, the coalescences due to a random collision and a wake entrainment are the dominant mechanisms as sink terms, whereas the breakup due to a turbulent impact has no role. However, as the liquid flow increases, the contribution from the breakup due to a turbulent impact becomes evident. As a further study, appropriate bubble interaction models, such as the shearing-off of a large bubble into small bubbles and a breakup due to a surface instability are to be developed for a slug flow regime.

Acknowledgement

This research has been performed under the nuclear R&D program supported by the Ministry of Science and Technology of the Korean Government.

References

[1] M. Ishii, Thermo-fluid Dynamic Theory of Two-Phase Flow, Eyrolles, Paris, Scientific and Medical Publication of France, New York, 1975.

[2] M. Ishii, Q. Wu, A. Assad, J. Uhle, Interfacial area transport equation for two-fluid model formulation, in : Proceedings of IMuST Meeting, 1998.

[3] S. Kalkach-Navarro, R.T. Lahey Jr., D.A. Drew, R. Meyder, Interfacial area density, mean radius and number density measurements in bubbly two-phase flow, Nucl. Eng. Des. 142 (1993) 341–351.

[4] G. Kocamustafaogullari, M. Ishii, Foundation of the interfacial area transport equation and its closure relations, Int. J. Heat Mass Transfer 38 (3) (1995) 481–493.

[5] Q. Wu, S. Kim, M. Ishii, S.G. Beus, One-Group interfacial area transport in vertical bubbly flow, Int. J. Heat Mass Transfer 41 (1998) 1103–1112.

[6] M. Millies, D.A. Mewes, Transport equation for the local interfacial area density in two-phase flows, in: Proceedings of the 2nd international conference on multiphase flow, Kyoto, Japan, 1995.

[7] M. Millies, D.A. Drew, R.T. Lahey Jr., A first order relaxation model for the prediction of the local interfacial area density in two-phase flows, Int. J. Multiphase Flow 22 (6) (1996) 1073–1104.

[8] T. Hibiki, M. Ishii, One-group interfacial area transport of bubbly flows in vertical round tubes, Int. J. Heat Mass Transfer 43 (2000) 2711–2726.

[9] T. Hibiki, M. Ishii, Two-Group interfacial area transport equations at bubbly-to-slug flow transition, Nucl. Eng. Des. 202 (2000) 39–76.

[10] Q. Wu, M. Ishii, Framework of two-group model for interfacial area transport in vertical two-phase flows, Trans. ANS 79 (1998) 351–352.

[11] X. Sun, M. Ishii, J.M. Kelly, Modified two-fluid model for the two-group interfacial area transport equation, Ann. Nucl. Energy 30 (2003) 1601–1622.

[12] F. Lehr, D. Mewes, A transport equation for the interfacial area density applied to bubble columns, Chem. Eng. Sci. 56 (2001) 1159–1166.

[13] D.J. Euh et al., Investigation of the transport of bubble parameters in air/water flow conditions, in: ICAPP05, Seoul, Korea, 2005.

[14] D.J. Euh et al., Development of the five sensor conductivity probe method for the measurement of interfacial area concentration, Nucl. Eng. Des. 205 (2001) 35–51.

[15] D.J. Euh et al., Numerical Simulation of an improved five-sensor probe method for local interfacial area concentration measurement, Nucl. Eng. Des. 234 (2004) 99–116.

[16] M.J. Prince et al., Bubble coalescence and break-up in air-sparged bubble columns, AIChE 36 (10) (1990) 1485–1499.

[17] C.A. Coulaloglou, L.L. Tavlarides, Description of interaction precesses in agitated liquid–liquid dispersions, Chem. Eng. Sci. 32 (1977) 1289–1297.

[18] R.D. Kirkpatrick, M.J. Lockett, The influence of approach velocity on bubble coalescence, Chem. Eng. Sci. 29 (1974) 2363–2373.

[19] V.G. Levich, Physicochemical Hydrodynamics, Prentice-Hall, Englewood Cliffs, NJ, 1962.

[20] H. Luo, H.F. Svendsen, Theoretical model for drop and bubble breakup in turbulent dispersions, AIChE 42 (5) (1996) 1225–1233.

[21] M. Ishii, N. Zuber, Drag coefficient and relative velocity in bubbly, droplet or particulate flows, AIChE J. 25 (1979) 843–855.

[22] T. Miyahara, K. Tsuchiya, L.S. Fan, Effect of turbulent wake on bubble-bubble interaction in a gas–liquid solid fluidized-bed, Chem. Eng. Sci. 46 (1991) 2368–2373.

[23] A.M.F.R. Pinto, M.N. Coelho Pinheiro, J.B.L.M. Campos, Coalescence of two gas slugs rising in a co-current flowing liquid in vertical tubes, Chem. Eng. Sci. 53 (1998) 2973–2983.

[24] A.M.F.R. Pinto, J.B.L.M. Campos, Coalescence of two gas slugs rising in a vertical column of liquid, Chem. Eng. Sci. 51 (1996) 45–54.

[25] R. Krishna, M.I. van Baten Urseanu, J. Ellenberger, Wall effects on the rise of single gas bubbles in liquids, Int. Commun. Heat Mass Transfer 26 (1999) 781–790.

[26] A.A. Amsden, F.H. Harlow, The SMAC method: a numerical technique for calculating incompressible fluid flow, Report LA-4370, Los Alamos Scientific Lab, 1971.